Receptor Signaling

Deutsche Ausgabe: DOI: 10.1002/ange.201508794
Internationale Ausgabe: DOI: 10.1002/anie.201508794

Identification of a Conformational Equilibrium That Determines the Efficacy and Functional Selectivity of the μ-Opioid Receptor

*Junya Okude, Takumi Ueda, Yutaka Kofuku, Motohiko Sato, Naoyuki Nobuyama, Keita Kondo, Yutaro Shiraishi, Takuya Mizumura, Kento Onishi, Mei Natsume, Masahiro Maeda, Hideki Tsujishita, Takefumi Kuranaga, Masayuki Inoue, and Ichio Shimada**

Abstract: *G-protein-coupled receptor (GPCR) ligands impart differing degrees of signaling in the G-protein and arrestin pathways, in phenomena called "biased signaling". However, the mechanism underlying the biased signaling of GPCRs is still unclear, although crystal structures of GPCRs bound to the G protein or arrestin are available. In this study, we observed the NMR signals from methionine residues of the μ-opioid receptor (μOR) in the balanced- and biased-ligand-bound states. We found that the intracellular cavity of μOR exists in an equilibrium between closed and multiple open conformations with coupled conformational changes on the transmembrane helices 3, 5, 6, and 7, and that the population of each open conformation determines the G-protein- and arrestin-mediated signaling levels in each ligand-bound state. These findings provide insight into the biased signaling of GPCRs and will be helpful for development of analgesics that stimulate μOR with reduced tolerance and dependence.*

G-protein-coupled receptors (GPCRs) are one of the largest membrane protein families in eukaryotes, and more than 30% of modern drugs target GPCRs. Drugs binding to GPCRs lead to the activation of signal transduction mediated by G proteins. Furthermore, the activated GPCRs are phosphorylated by GPCR kinases (GRKs), and the phosphorylated GPCRs stimulate G-protein-independent signal transduction mediated by arrestin.

GPCR ligands promote differing degrees of signaling in the G-protein and arrestin pathways, in phenomena called "functional selectivity" or "biased signaling",[1] and the ligands that promote both of the signaling pathways and those that preferably promote one of the signaling pathways are referred to as "balanced ligands" and "biased ligands", respectively. In the case of the μ-opioid receptor (μOR),[2] a class A GPCR stimulated by various opioid drugs, such as morphine, stimulation by TRV130[3] elicits signaling through Gi, the inhibitory G protein for adenylyl cyclase, but markedly reduces signaling through β-arrestin.[4] Furthermore, the $N131^{3.35}A$ and $N131^{3.35}V$ mutants (superscripts indicate Ballesteros–Weinstein numbers[5]) of the δ-opioid receptor constitutively activate β-arrestin-mediated signaling.[6]

μOR signaling through the G protein and that through β-arrestin are responsible for its analgesic properties[7] and adverse effects,[8] respectively, and TRV130 reportedly increases analgesia and reduces on-target adverse effects versus morphine.[4,9] Potential therapeutic applications of the functional selectivity of various GPCRs have also been proposed.[10] Therefore, the mechanisms underlying the functional selectivity of μOR are important for understanding the functions of GPCRs and for drug development.

Crystal structures of GPCRs in various forms have been solved, including GPCRs bound to inverse agonists and a GPCR bound to a full agonist with a G protein or a G-protein-mimicking nanobody[11] (see the Supporting Information). Furthermore, a crystal structure of rhodopsin bound to visual arrestin was recently reported.[12] However, this structure cannot explain the functional selectivity of the receptor, because the conformation of rhodopsin is almost identical to that in the crystal structure of rhodopsin bound to a peptide variant of the C terminus of G-transducin.[13] Therefore, we utilized NMR spectroscopy to clarify the conformational equilibrium of μOR in the states bound to an antagonist, balanced agonists, and TRV130.

We prepared μORs with the sequences Gly54–Gln362 and Gly54–Pro400, both with the $F158^{3.41}W$ mutation, in 2,2-didecylpropane-1,3-bis-β-D-maltopyranoside (LMNG) micelles and those reconstituted into the lipid bilayer of reconstituted high-density lipoproteins (rHDLs),[14,15] also known as nanodiscs,[16] were prepared (see Figure S1 and details in the Supporting Information). Hereafter, the obtained μORs (Gly54–Gln362)/$F158^{3.41}W$ and (Gly54–Pro400)/$F158^{3.41}W$ are referred to as μOR-A and μOR-A′, respectively. The obtained μOR retained binding activity to naloxone, morphine, DAMGO, and TRV130 (see Figures S2–S5 and details in the Supporting Information).

Our analysis of the G-protein and β-arrestin signaling efficacies of μOR bound to various ligands revealed that

[*] Dr. J. Okude, Dr. T. Ueda, Dr. Y. Kofuku, M. Sato, N. Nobuyama, K. Kondo, Y. Shiraishi, T. Mizumura, K. Onishi, M. Natsume, Dr. T. Kuranaga, Prof. Dr. M. Inoue, Prof. Dr. I. Shimada
Graduate School of Pharmaceutical Sciences, The University of Tokyo
Hongo 7-3-1, Bunkyo-ku, Tokyo 113-0033 (Japan)
E-mail: shimada@iw-nmr.f.u-tokyo.ac.jp
Dr. T. Ueda
Precursory Research for Embryonic Science and Technology (PRESTO), Japan Science and Technology Agency (JST)
Chiyoda-ku, Tokyo 102-0075 (Japan)
Dr. M. Maeda, Dr. H. Tsujishita
Shionogi Co., Ltd., Discovery Research Laboratories
Osaka 561-0825 (Japan)

Supporting information for this article is available on the WWW under http://dx.doi.org/10.1002/anie.201508794.

naloxone, morphine, DAMGO, and TRV130 are the antagonist, balanced partial agonist, balanced full agonist, and G-protein-biased partial agonist, respectively, against μOR with the F158$^{3.41}$W mutation, which was used in the NMR spectroscopic analysis, and that the N152$^{3.35}$A mutant is a β-arrestin-biased mutant (Figure 1; see also Figure S6 and

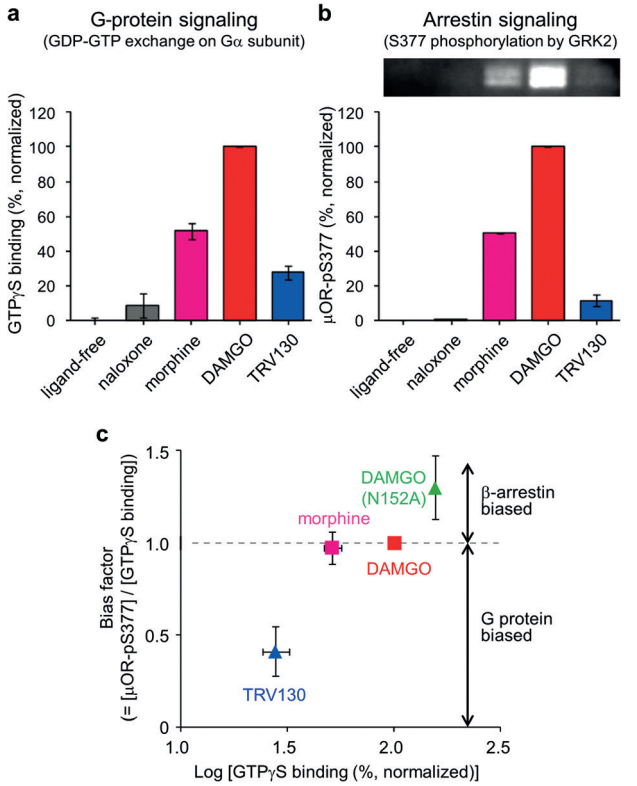

Figure 1. Efficacy and bias factors of μOR and μOR/N152$^{3.35}$A in the presence of each ligand. a,b) Activation of G-protein- and β-arrestin signaling by μOR-A′ in rHDLs. a) [^{35}S]GTPγS binding to complexes of purified G protein/μOR-A′ in rHDLs with various ligands. Results are expressed as a percentage with respect to the binding stimulated by DAMGO. b) GRK2-mediated phosphorylation at S377 of μOR-A′ bound to naloxone, morphine, DAMGO, and TRV130 in rHDLs, as detected by western blotting with an anti-phosphorylated S377 antibody. A gel image is shown at the top. Results are expressed as a percentage with respect to the phosphorylation of μOR-A′ bound to DAMGO. Data are the mean ± standard error of the mean of triplicate determinations from three separate representative experiments. c) Bias factor, which is the ratio of the β-arrestin signaling efficacy (b; see also Figure S7b) to the G-protein signaling efficacy (a; see also Figure S7a), for different ligands relative to that of DAMGO against μOR without the N152$^{3.35}$A mutation versus the logarithm of [^{35}S]GTPγS binding (a; see Figure S7a). We could not accurately determine the bias factor of μOR stimulated by naloxone, because the G-protein and β-arrestin efficacies were both low.

details in the Supporting Information). These results are in agreement with those from previous studies on μOR without the F158$^{3.41}$W mutation.[4,17]

μOR-A possesses 13 methionine residues in TM1-6, extracellular loop 2 (ECL2), intracellular loop 1 (ICL1), and ICL3 (see Figure S7). M163$^{3.46}$, M245$^{5.49}$, M257$^{5.61}$, and M283$^{6.36}$ exist on the intracellular side of TM3, 5, and 6, and the side chains of M163$^{3.46}$ and M283$^{6.36}$ are directed toward TM7. These methionine residues should be good probes to investigate the ligand-induced conformational changes, considering that TM3, TM5, TM6, and TM7 assume distinctly different conformations upon GPCR activation.[11] In the ^{1}H–^{13}C methyl transverse relaxation-optimized spectroscopy (TROSY) spectra of [αβ-^{2}H-,methyl-^{13}C-Met]μOR-A in LMNG micelles in the balanced-full-agonist (DAMGO)-bound and the antagonist (naloxone)-bound states, severely overlapped resonances that apparently originated from the methionine residues were observed (see Figure S8a,b). To overcome the problem of signal overlap, we introduced mutations into the solvent- or lipid-exposed methionine residue (see Figure S9a).[18] Hereafter, we refer to the resulting M67$^{1.29}$L/M74$^{1.36}$T/M132$^{2.66}$L/M205$^{4.61}$I/M207^{ECL2}L/M266^{ICL3}L mutant as μOR-Δ6M. The G-protein signaling was not affected by the Δ6M mutation or the truncation of the C terminus (Figure 1a; see also Figure S9b). To overcome the problem of the broadening of several resonances owing to ^{1}H–^{1}H dipole interactions between the observed and surrounding ^{1}H atoms, we utilized the recently developed deuteration method for proteins expressed in an insect-cell–baculovirus expression system[14] (see Figures S10–S12 and details in the Supporting Information). Hereafter, the obtained μOR-A/Δ6M mutant, in which eight types of amino acid residues (isoleucine, leucine, phenylalanine, lysine, arginine, threonine, valine, and tyrosine residues) were deuterated, is referred to as [^{2}H-8AA, αβ-^{2}H-,methyl-^{13}C-Met]μOR-A/Δ6M. In the methyl-TROSY spectra of [^{2}H-8AA, αβ-^{2}H-,methyl-^{13}C-Met]μOR-A/Δ6M, signals that apparently originated from the seven methionine residues of μOR-A/Δ6M were detected, thus suggesting that most of the methionine residues were observed (see Figure S8c,d). Several methionine resonances were not clearly observed in the spectra of μOR-A/Δ6M without deuteration (see Figure S12), thus suggesting that the sensitivity for these resonances was increased more than threefold upon deuteration.

Assignments of the methionine resonances were established by comparison of the spectra of difference mutants (see Figures S13–S15 and details in the Supporting Information). Crystal structures of μOR indicate that the ^{1}H chemical shifts of the resonances from M245$^{5.49}$ would be sensitive to the conformational changes of TM5 upon activation (see Figure S16 and details in the Supporting Information). The ^{1}H and ^{13}C chemical shifts of the major M245$^{5.49}$ signal in the antagonist-bound state was markedly different from that for the balanced-full-agonist-bound state (Figure 2a). Hereafter, the major signals in the inactive antagonist- and active full-agonist-bound states are referred to as M245^{I} and M245^{A}, respectively.

To investigate the structures of the μOR TM region that elicits partially activated signaling, we recorded the ^{1}H-^{13}C methyl-TROSY spectra of [^{2}H-8AA, αβ-^{2}H-,methyl-^{13}C-Met]μOR-A/Δ6M in the balanced-partial-agonist (morphine)-bound state. Two resonances, the chemical shifts of which were almost identical to those of the M245^{I} and M245^{A} resonances, were observed (Figure 2a). The relative intensities of the two resonances with chemical shifts almost identical to those of M245^{I} and M245^{A} in the antagonist-,

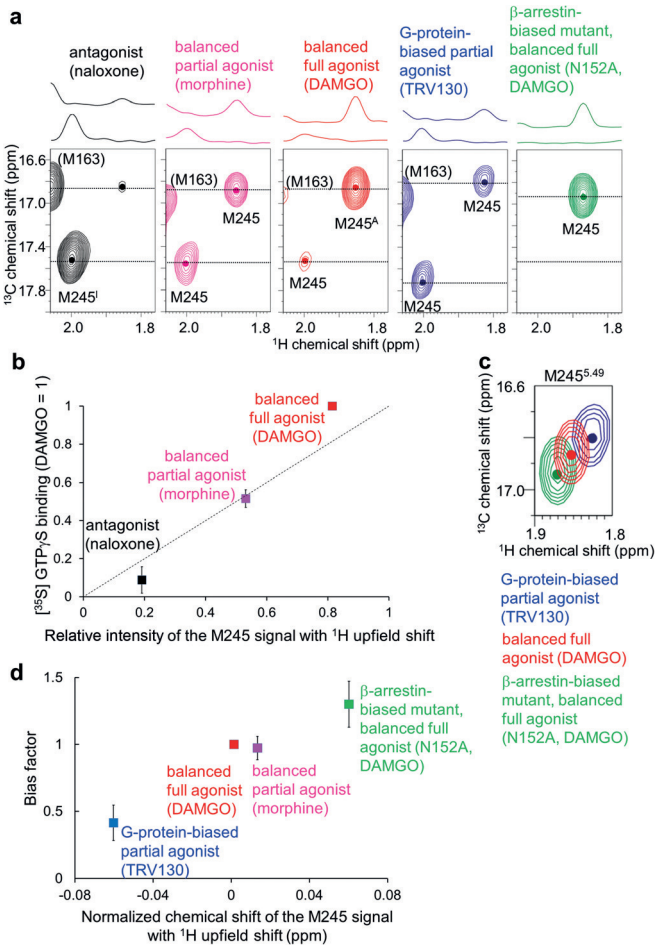

Figure 2. Difference in the μOR M245$^{5.49}$ resonances in states with various efficacies and bias factors. a) ^{1}H–^{13}C HMQC spectra of the [^{2}H-8AA, αβ-^{2}H-,methyl-^{13}C-Met]μOR-A/Δ6M mutant in the naloxone-bound (black), morphine-bound (magenta), DAMGO-bound (red), and TRV130-bound states (blue) and that of the μOR-A/Δ6M/N152$^{3.35}$A mutant in the DAMGO-bound state (green). Cross-sections at the dashed gray lines are shown above the spectra. b) Correlation between the relative intensities of the M245$^{5.49}$ signals and the activation of G-protein signaling. Plot of [^{35}S]GTPγS binding to the complex of μOR-A′ in rHDLs and heterotrimeric G protein with each ligand versus the ratio of the intensity of the resonance with ^{1}H and ^{13}C chemical shifts almost identical to that of M245^{A}, relative to the sum of the intensities of the two M245$^{5.49}$ signals. The dotted line represents the points at which the relative [^{35}S]GTPγS binding is equal to the relative intensity of the resonances with chemical shifts almost identical to that of M245^{A}. c) Overlay of the spectra shown (a), except for the μOR-A/Δ6M mutant in the naloxone-bound and morphine-bound states. Only the region with the M245$^{5.49}$ resonance is shown. The centers of the resonances from M245$^{5.49}$ are indicated with dots. d) Correlation between the normalized chemical shift of the M245$^{5.49}$ signal with an ^{1}H upfield shift and the bias factor. The normalized chemical shifts were calculated from the formula $[(\delta_{^1H}-\delta_{^1H}(\mathrm{TRV130}))^2+\{(\delta_{^{13}C}-\delta_{^{13}C}(\mathrm{TRV130}))/3.5\}^2]-[(\delta_{^1H}-\delta_{^1H}(\mathrm{N152A}))^2+\{(\delta_{^{13}C}-\delta_{^{13}C}(\mathrm{N152A}))/3.5\}^2]^{0.5}$, in which $\delta_{^1H}$(TRV130) and $\delta_{^{13}C}$(TRV130) are the ^{1}H and ^{13}C chemical shifts in the TRV130-bound state, and $\delta_{^1H}$(N152A) and $\delta_{^{13}C}$(N152A) are the ^{1}H and ^{13}C chemical shifts of the β-arrestin-biased mutant in the DAMGO-bound state.

balanced-partial-agonist-, and balanced-full-agonist-bound states correlated well with [^{35}S]GTPγS binding to the complex of μOR and the G protein in the presence of each ligand (Figure 2b). The efficacy-dependent signal intensities of M245$^{5.49}$, together with the previous structural analyses of GPCRs (see the Supporting Information), indicate that μOR exists in an equilibrium between the closed and open conformations, which correspond to M245^{I} and M245^{A}, respectively, with slower exchange rates than the chemical-shift difference ($<200\ s^{-1}$), and that the population of the open conformations determines the activation of the G-protein signaling level. The slow exchange rates are in agreement with those of the equilibrium between the closed and open conformations of β_2AR in LMNG micelles.[19]

To investigate the structures of the μOR TM region that elicits biased signaling, we recorded ^{1}H–^{13}C methyl-TROSY spectra of [^{2}H-8AA, αβ-^{2}H-,methyl-^{13}C-Met]μOR-A/Δ6M in the G-protein-biased-partial-agonist (TRV130)-bound state and the β-arrestin-biased mutant (μOR-A/Δ6M/N152$^{3.35}$A) in the balanced-full-agonist-bound state. For the G-protein-biased-partial-agonist-bound state, two resonances that were remarkably shifted from M245^{I} and M245^{A} were observed (Figure 2a,c). In the spectrum of the β-arrestin-biased mutant bound to the full agonist, one resonance, which was remarkably shifted from M245^{A}, was observed (Figure 2a,c). The ^{1}H and ^{13}C chemical shifts of M245^{A} were between those observed in the G-protein-biased-partial-agonist-bound state and the β-arrestin-biased mutant bound to the full agonist (Figure 2c), and the chemical shifts of M245 correlated well with the bias factors in each state (Figure 2d). To examine whether the resonances from M245$^{5.49}$ in the balanced-full-agonist-bound state underwent conformational exchange, we recorded the spectra of μOR-A at the lower temperature of 283 K (see Figure S17). In this case, the M245$^{5.49}$ resonance significantly shifted away from that for the G-protein-biased-partial-agonist-bound state. These results suggest that μOR exists in an equilibrium between multiple open conformations, including the conformations that preferentially activate either G-protein-mediated signaling or β-arrestin-mediated signaling, with faster exchange rates than the chemical-shift difference ($>100\ s^{-1}$), and that the equilibrium is shifted toward the former and latter conformations in the G-protein-biased-ligand-bound state and the full-agonist-bound state of the β-arrestin-biased mutant, respectively.

M163$^{3.46}$, M257$^{5.61}$, and M283$^{6.36}$ exist in the intracellular side of TM3, TM5, and TM6 (see Figure S7), and their chemical shifts would be sensitive to conformational changes of TM7, as well as TM3, TM5, and TM6 (see Figure S18 and details in the Supporting Information). The chemical shifts of M283$^{6.36}$ indicate that the resonances observed in the antagonist- and full-agonist-bound states correspond to the closed and open conformations, respectively (see the Supporting Information). Furthermore, the chemical shifts of the M163$^{3.46}$, M257$^{5.61}$, and M283$^{6.36}$ signals in the balanced-full-agonist-bound state were also between those for the G-protein-biased-partial-agonist-bound state and those for the full-agonist-bound state with the β-arrestin-biased mutation (Figure 3a; see also Figures S19–S23 and details in the Supporting Information). Therefore, the efficacy- and bias-factor-dependent conformational equilibrium observed for M245$^{5.49}$ accompanies the coupled conformational changes on

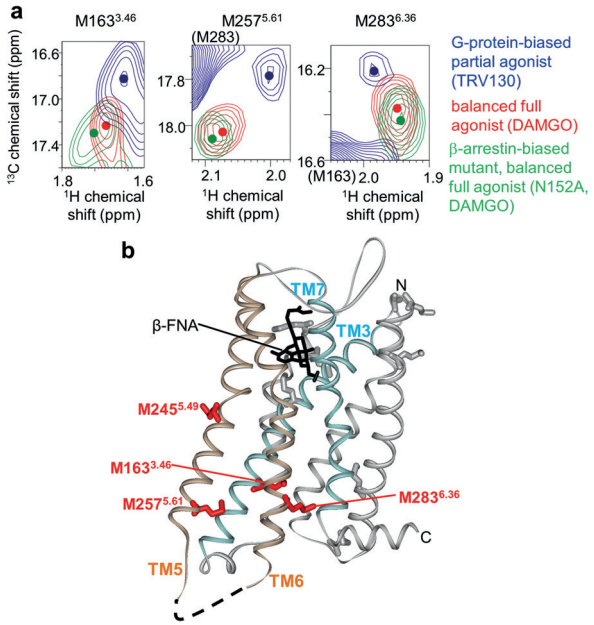

Figure 3. Distribution of the methionine residues that exhibited chemical shifts in a functional-selectivity-dependent manner. a) Overlaid ^{1}H–^{13}C HMQC spectra of the [^{2}H-8AA, αβ-^{2}H-,methyl-^{13}C-Met]μOR-A/Δ6M/M245$^{5.49}$V mutant in the DAMGO-bound (red) and TRV130-bound states (blue) and that of μOR-A/Δ6M/M245$^{5.49}$V/N152$^{3.35}$A mutant in the DAMGO-bound state (green). Only the regions with M257$^{5.61}$, M283$^{6.36}$, and M163$^{3.46}$ resonances are shown. The centers of the resonances from M163$^{3.46}$, M257$^{5.61}$, and M283$^{6.36}$ are indicated with dots. b) Mapping of the methionine residues that exhibited chemical shifts in a functional-selectivity-dependent manner. The crystal structure of μOR in a complex with an irreversible antagonist, β-funaltrexamine (PDB accession code: 4DKL), is shown as a white ribbon model, and M163$^{3.46}$, M245$^{5.49}$, M257$^{5.61}$, and M283$^{6.36}$, which exhibited chemical shifts in a functional-selectivity-dependent manner (Figure 2b,c), are depicted by red sticks. The other methionine residues and β-funaltrexamine are depicted by white and black sticks, respectively. TM3/7 and TM5/6 are colored cyan and light orange, respectively.

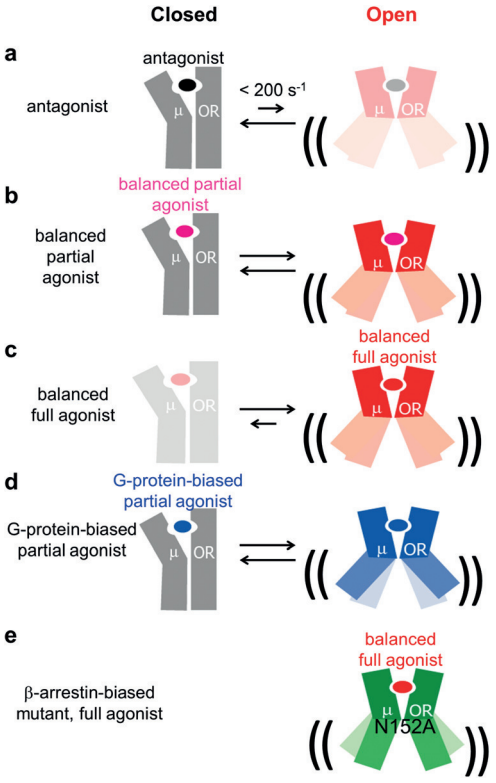

Figure 4. Proposed mechanism for the differences in the efficacy and functional selectivity of μOR for different ligands. In the antagonist (naloxone)-bound state (a), μOR primarily adopts the closed conformation. In the balanced-partial-agonist (morphine)-bound state (b), μOR exists in equilibrium between the closed and open conformations. In the balanced-full-agonist (DAMGO)-bound state (c), μOR primarily adopts the open conformation. In the aforementioned balanced-ligand-bound states, the intracellular side exists in equilibrium between multiple conformations. In the G-protein-biased-partial-agonist (TRV130)-bound state (d), μOR exists in equilibrium between the closed and open conformations, and the equilibrium within the open conformation is shifted toward the conformation with a larger intracellular cavity. In the DAMGO-bound state of the μOR N152$^{3.35}$A mutant (e), μOR adopts the open conformation, and the equilibrium within the open conformation is shifted toward the conformation with a smaller intracellular cavity.

the intracellular side of TM3, TM5, TM6, and TM7 (Figure 3b). The biased signaling of μOR by the coupled conformational changes on TM3, TM5, TM6, and TM7 is in contrast to the previously reported selective activation of G-protein- and β-arrestin-mediated signaling by decoupled conformational changes of TM5/6 and TM3/7, respectively, in other GPCRs.[20,21] It is possible that the intracellular cavity, which is formed in the crystal structure of GPCRs bound to a full agonist with a G protein or G-protein-mimicking nanobody,[11] is relatively small in the conformation that preferentially activates β-arrestin signaling (see the Supporting Information).

On the basis of our structural interpretation of the M245$^{5.49}$ resonances, we propose the following signal-regulation mechanism (Figure 4): In the antagonist (naloxone)-bound state, μOR primarily adopts the closed conformation. In the balanced-full-agonist (DAMGO)-bound state, μOR primarily adopts the open conformation, and the intracellular cavity, which is composed of TM3, TM5, TM6, and TM7, exists in equilibrium between multiple open conformations, including the conformations that preferentially activate either G-protein-mediated signaling or β-arrestin-mediated signaling. In the balanced-partial-agonist (morphine)-bound state, μOR exists in equilibrium between the aforementioned closed and multiple open conformations. In the G-protein-biased-partial-agonist (TRV130)-bound state, μOR exists in equilibrium between the closed and multiple open conformations, and the equilibrium between the multiple open conformations is shifted toward the conformation that preferentially activates G-protein-mediated signaling. In the DAMGO-bound state of the μOR N152$^{3.35}$A mutant, μOR adopts the open conformation, and the equilibrium between the multiple open conformations is shifted toward the conformations that preferentially activate β-arrestin-mediated signaling. The dynamic characteristics of μOR are in agreement with the fast dynamics of another GPCR observed in recent solid-state NMR studies.[22]

The conformational equilibrium that accompanies the coupled conformational change in TM3, TM5, TM6, and TM7

upon the introduction of the β-arrestin-biased N152A mutation is in agreement with the structure–activity relationships of TRV130 derivatives (see Figure S24 and details in the Supporting Information). TRV130 reportedly produced greater analgesia than morphine, at doses with less reduction in respiratory drive and diminished nausea in healthy human volunteers.[9] Therefore, observation of the population shift of the conformational equilibrium of μOR bound to various ligands, on the basis of the M245$^{5.49}$ resonances, would be helpful for the further development of analgesics with reduced side effects, better tolerance, and negligible dependence.

It is possible that the functional selectivity of other GPCRs is also regulated by the population shift of the conformational equilibrium that accompanies the coupled conformational changes of TM3, TM5, TM6, and TM7, as well as μOR (see the Supporting information). Therefore, the conformational equilibrium in the transmembrane region is important for understanding the functional selectivity of GPCRs. Observation of the NMR signals of methionine residues, which are highly abundant in TM helices of GPCRs and can be observed without any chemical modification,[18] is applicable for the analysis of the conformational equilibrium that regulates biased signaling in various GPCRs.

In previous NMR studies of GPCRs, the conformational changes of GPCRs induced by biased ligands or G-protein-mimicking nanobodies were observed by the use of ^{19}F and $^{13}CH_3$ probes chemically attached to cysteine and lysine residues, respectively.[20,23] In these studies, the chemical probes could not be attached to residues in the middle of the transmembrane region owing to their solvent inaccessibility, although the residues that are widely conserved and exhibit remarkable conformational changes upon activation, such as the P$^{5.50}$–I$^{3.40}$–F$^{6.44}$ trigger motif and the NP$^{7.50}$xxY motif, exist in the middle of the transmembrane region. Furthermore, there is a possibility that the probe would reflect the perturbation of the local conformation by the chemical modification. In contrast, methionine-selective labeling enabled the direct observation of the residues in the transmembrane region without any perturbation of the local conformation.[14,18,24] Deuteration also enabled the observation of the transmembrane region of μOR in the present study (see Figure S12), even at a low μOR concentration (5–10 μM). Therefore, methionine-selective labeling, along with deuteration, should be useful for the analysis of the conformational dynamics of the transmembrane regions of GPCRs and other membrane proteins.

In this study, our NMR analysis of μOR in the balanced- and biased-ligand-bound states revealed that the intracellular cavity of μOR exists in an equilibrium between closed and multiple open conformations, and that the population of each open conformation determines the G-protein- and β-arrestin-mediated signaling levels in each ligand-bound state. These findings provide structural insight into the biased signaling of μOR and other GPCRs.

Acknowledgements

We thank Dr. Atsushi Kimishima and Dr. Tohru Fukuyama for the preparation of morphine derivatives. This research was supported in part by grants from the Japan New Energy and Industrial Technology Development Organization (NEDO) and the Ministry of Economy, Trade and Industry (METI), and by a Grant-in-Aid for Scientific Research on Priority Areas from the Japanese Ministry of Education, Culture, Sports, Science and Technology (MEXT).

Keywords: G-protein-coupled receptors · isotopic labeling · lipid bilayers · membrane proteins · NMR spectroscopy

How to cite: *Angew. Chem. Int. Ed.* **2015**, *54*, 15771–15776
Angew. Chem. **2015**, *127*, 15997–16002

[1] E. Reiter, S. Ahn, A. K. Shukla, R. J. Lefkowitz, *Annu. Rev. Pharmacol. Toxicol.* **2012**, *52*, 179–197.
[2] H. W. Matthes, R. Maldonado, F. Simonin, O. Valverde, S. Slowe, I. Kitchen, K. Befort, A. Dierich, M. Le Meur, P. Dolle, E. Tzavara, J. Hanoune, B. P. Roques, B. L. Kieffer, *Nature* **1996**, *383*, 819–823; J. A. Lord, A. A. Waterfield, J. Hughes, H. W. Kosterlitz, *Nature* **1977**, *267*, 495–499.
[3] X. T. Chen, P. Pitis, G. Liu, C. Yuan, D. Gotchev, C. L. Cowan, D. H. Rominger, M. Koblish, S. M. Dewire, A. L. Crombie, J. D. Violin, D. S. Yamashita, *J. Med. Chem.* **2013**, *56*, 8019–8031.
[4] S. M. DeWire, D. S. Yamashita, D. H. Rominger, G. Liu, C. L. Cowan, T. M. Graczyk, X. T. Chen, P. M. Pitis, D. Gotchev, C. Yuan, M. Koblish, M. W. Lark, J. D. Violin, *J. Pharmacol. Exp. Ther.* **2013**, *344*, 708–717.
[5] J. A. Ballesteros, H. Weinstein, *Methods Neurosci.* **1995**, *25*, 366–428.
[6] G. Fenalti, P. M. Giguere, V. Katritch, X. P. Huang, A. A. Thompson, V. Cherezov, B. L. Roth, R. C. Stevens, *Nature* **2014**, *506*, 191–196.
[7] R. B. Raffa, R. P. Martinez, C. D. Connelly, *Eur. J. Pharmacol.* **1994**, *258*, R5–7.
[8] L. M. Bohn, R. J. Lefkowitz, R. R. Gainetdinov, K. Peppel, M. G. Caron, F. T. Lin, *Science* **1999**, *286*, 2495–2498.
[9] D. G. Soergel, R. A. Subach, N. Burnham, M. W. Lark, I. E. James, B. M. Sadler, F. Skobieranda, J. D. Violin, L. R. Webster, *Pain* **2014**, *155*, 1829–1835; D. G. Soergel, R. A. Subach, B. Sadler, J. Connell, A. S. Marion, C. L. Cowan, J. D. Violin, M. W. Lark, *J. Clin. Pharmacol.* **2014**, *54*, 351–357.
[10] J. A. Allen, B. L. Roth, *Annu. Rev. Pharmacol. Toxicol.* **2011**, *51*, 117–144; T. Kenakin, C. Watson, V. Muniz-Medina, A. Christopoulos, S. Novick, *ACS Chem. Neurosci.* **2012**, *3*, 193–203.
[11] V. Cherezov, D. M. Rosenbaum, M. A. Hanson, S. G. Rasmussen, F. S. Thian, T. S. Kobilka, H. J. Choi, P. Kuhn, W. I. Weis, B. K. Kobilka, R. C. Stevens, *Science* **2007**, *318*, 1258–1265; S. G. Rasmussen, B. T. DeVree, Y. Zou, A. C. Kruse, K. Y. Chung, T. S. Kobilka, F. S. Thian, P. S. Chae, E. Pardon, D. Calinski, J. M. Mathiesen, S. T. Shah, J. A. Lyons, M. Caffrey, S. H. Gellman, J. Steyaert, G. Skiniotis, W. I. Weis, R. K. Sunahara, B. K. Kobilka, *Nature* **2011**, *477*, 549–555; A. Manglik, A. C. Kruse, T. S. Kobilka, F. S. Thian, J. M. Mathiesen, R. K. Sunahara, L. Pardo, W. I. Weis, B. K. Kobilka, S. Granier, *Nature* **2012**, *485*, 321–326; W. Huang, A. Manglik, A. J. Venkatakrishnan, T. Laeremans, E. N. Feinberg, A. L. Sanborn, H. E. Kato, K. E. Livingston, T. S. Thorsen, R. C. Kling, S. Granier, P. Gmeiner, S. M. Husbands, J. R. Traynor, W. I. Weis, J. Steyaert, R. O. Dror, B. K. Kobilka, *Nature* **2015**, *524*, 315–321.
[12] Y. Kang, X. E. Zhou, X. Gao, Y. He, W. Liu, A. Ishchenko, A. Barty, T. A. White, O. Yefanov, G. W. Han, Q. Xu, P. W. de Waal,

J. Ke, M. H. Tan, C. Zhang, A. Moeller, G. M. West, B. D. Pascal, N. Van Eps, L. N. Caro, S. A. Vishnivetskiy, R. J. Lee, K. M. Suino-Powell, X. Gu, K. Pal, J. Ma, X. Zhi, S. Boutet, G. J. Williams, M. Messerschmidt, C. Gati, N. A. Zatsepin, D. Wang, D. James, S. Basu, S. Roy-Chowdhury, C. E. Conrad, J. Coe, H. Liu, S. Lisova, C. Kupitz, I. Grotjohann, R. Fromme, Y. Jiang, M. Tan, H. Yang, J. Li, M. Wang, Z. Zheng, D. Li, N. Howe, Y. Zhao, J. Standfuss, K. Diederichs, Y. Dong, C. S. Potter, B. Carragher, M. Caffrey, H. Jiang, H. N. Chapman, J. C. Spence, P. Fromme, U. Weierstall, O. P. Ernst, V. Katritch, V. V. Gurevich, P. R. Griffin, W. L. Hubbell, R. C. Stevens, V. Cherezov, K. Melcher, H. E. Xu, *Nature* **2015**, *523*, 561 – 567.

[13] J. Standfuss, P. C. Edwards, A. D'Antona, M. Fransen, G. Xie, D. D. Oprian, G. F. Schertler, *Nature* **2011**, *471*, 656 – 660.

[14] Y. Kofuku, T. Ueda, J. Okude, Y. Shiraishi, K. Kondo, T. Mizumura, S. Suzuki, I. Shimada, *Angew. Chem. Int. Ed.* **2014**, *53*, 13376 – 13379; *Angew. Chem.* **2014**, *126*, 13594 – 13597.

[15] C. Yoshiura, Y. Kofuku, T. Ueda, Y. Mase, M. Yokogawa, M. Osawa, Y. Terashima, K. Matsushima, I. Shimada, *J. Am. Chem. Soc.* **2010**, *132*, 6768 – 6777.

[16] T. H. Bayburt, Y. V. Grinkova, S. G. Sligar, *Nano Lett.* **2002**, *2*, 853 – 856.

[17] J. McPherson, G. Rivero, M. Baptist, J. Llorente, S. Al-Sabah, C. Krasel, W. L. Dewey, C. P. Bailey, E. M. Rosethorne, S. J. Charlton, G. Henderson, E. Kelly, *Mol. Pharmacol.* **2012**, *78*, 756 – 766.

[18] Y. Kofuku, T. Ueda, J. Okude, Y. Shiraishi, K. Kondo, M. Maeda, H. Tsujishita, I. Shimada, *Nat. Commun.* **2012**, *3*, 1045.

[19] K. Y. Chung, T. H. Kim, A. Manglik, R. Alvares, B. K. Kobilka, R. S. Prosser, *J. Biol. Chem.* **2012**, *287*, 36305 – 36311.

[20] J. J. Liu, R. Horst, V. Katritch, R. C. Stevens, K. Wüthrich, *Science* **2012**, *335*, 1106 – 1110.

[21] D. Wacker, C. Wang, V. Katritch, G. W. Han, X. P. Huang, E. Vardy, J. D. McCorvy, Y. Jiang, M. Chu, F. Y. Siu, W. Liu, H. E. Xu, V. Cherezov, B. L. Roth, R. C. Stevens, *Science* **2013**, *340*, 615 – 619.

[22] P. Schmidt, L. Thomas, P. Müller, H. A. Scheidt, D. Huster, *Chem. Eur. J.* **2014**, *20*, 4986 – 4992; L. Thomas, J. Kahr, P. Schmidt, U. Krug, H. A. Scheidt, D. Huster, *J. Biomol. NMR* **2015**, *61*, 347 – 359.

[23] M. P. Bokoch, Y. Zou, S. G. Rasmussen, C. W. Liu, R. Nygaard, D. M. Rosenbaum, J. J. Fung, H. J. Choi, F. S. Thian, T. S. Kobilka, J. D. Puglisi, W. I. Weis, L. Pardo, R. S. Prosser, L. Mueller, B. K. Kobilka, *Nature* **2010**, *463*, 108 – 112; A. Manglik, T. H. Kim, M. Masureel, C. Altenbach, Z. Yang, D. Hilger, M. T. Lerch, T. S. Kobilka, F. S. Thian, W. L. Hubbell, R. S. Prosser, B. K. Kobilka, *Cell* **2015**, *161*, 1101 – 1111; R. Sounier, C. Mas, J. Steyaert, T. Laeremans, A. Manglik, W. Huang, B. K. Kobilka, H. Déméné, S. Granier, *Nature* **2015**, *524*, 375 – 378.

[24] R. Nygaard, Y. Zou, R. O. Dror, T. J. Mildorf, D. H. Arlow, A. Manglik, A. C. Pan, C. W. Liu, J. J. Fung, M. P. Bokoch, F. S. Thian, T. S. Kobilka, D. E. Shaw, L. Mueller, R. S. Prosser, B. K. Kobilka, *Cell* **2013**, *152*, 532 – 542.

Received: September 19, 2015
Revised: October 19, 2015
Published online: November 16, 2015

